

*In celebration of the 60<sup>th</sup> birthday of Dr. Andrew K. Galwey*

## **NON-ISOTHERMAL DECOMPOSITION OF SILVER MALEATE DIHYDRATE AND ANHYDROUS SILVER FUMARATE**

*M. A. Mohamed\*<sup>1</sup>, S. A. A. Mansour<sup>2</sup> and G. A. M. Hussien<sup>2</sup>*

<sup>1</sup>Chemistry Department, Faculty of Science, Qena, Egypt

<sup>2</sup>Chemistry Department, Faculty of Science, Minia University, El-Minia 61519, Egypt

### **Abstract**

The non-isothermal decompositions of silver maleate dihydrate ( $C_4H_2O_4Ag_2 \cdot 2H_2O$ ) and anhydrous silver fumarate ( $C_4H_2O_4Ag_2$ ) were studied up to 500°C, in a dynamic atmosphere of air, by means of TG and DTA measurements. Both compounds showed some sublimation (at 120°C for silver maleate and at 180°C for silver fumarate) prior to the onset of decomposition (at 170°C for silver maleate and at 280°C for silver fumarate).

The gaseous decomposition products of both compounds were found, using IR spectroscopy, to be dominated by maleic anhydride and CO<sub>2</sub>. Minor proportions of ethylene, ethyl alcohol, acetone, methane and isobutene were also identified. Metallic silver was the final solid product, as identified by X-ray diffractometry. NMR analysis was used to monitor the isomerization of the maleate radical into the more stable fumarate above 230°C. Kinetic parameters ( $E_a$  and  $\ln A$ ) were calculated from the effect of heating rate (2, 5, 10, and 20 deg·min<sup>-1</sup>) on the DTA measurements.

A mechanism is suggested for the decomposition pathways of these compounds, on basis of the results obtained and, also, on similarities with analogous systems.

**Keywords:** anhydrous silver fumarate, kinetics, NMR analysis, silver maleate dihydrate, TG-DTA, X-ray

### **Introduction**

The thermal decompositions of metal carboxylates have been the subject of several kinetic and mechanistic studies, using either conventional isothermal techniques or one of the many non-isothermal methods [1]. Silver carboxylates are amongst the most extensively studied materials. Silver formate was shown

---

\* To whom correspondence should be addressed

[2] to explode, with intensive detonation, on heating to 92°C. H<sub>2</sub> and CO were the main gaseous products and Ag<sup>0</sup> metal was the eventual solid residue. The kinetics of silver oxalate decomposition were found to be sensitive to a number of factors, including the method of preparation [3], doping [4], aging, grinding and pre-irradiation [5, 6]. The decomposition was suggested [7] to proceed via an electron-transfer mechanism, giving rise to CO<sub>2</sub> gas and Ag metal.

The decomposition of silver malonate was studied isothermally [8]. The results suggested a nucleation-and-growth mechanism. CO<sub>2</sub>, CO and acetic acid were identified as volatile decomposition products, while carbon and Ag<sup>0</sup> were the solid products. Pre-irradiation with  $\gamma$ -rays was found [9] to shorten the induction period to onset of decomposition. Silver squarate was studied both isothermally and non-isothermally [10, 11]. CO<sub>2</sub>, CO and Ag<sup>0</sup> metal were the decomposition products. The mechanism suggested proposes the formation of Ag<sub>2</sub>O as a reaction intermediate [11]. Silver mellitate has been reported [12] to decompose via a nucleation-and-growth mechanism, and CO<sub>2</sub>, CO, Ag<sup>0</sup> and carbon were the products identified.

Only a very few studies have been concerned with the decomposition of metal maleates and fumarates; these were of nickel and copper. Decomposition in vacuum of nickel maleate [13] yields nickel and carbon residues between 270–310°C, while nickel fumarate [14] decomposes at slightly higher temperatures (300–340°C), to give Ni<sub>3</sub>C. Taki *et al.* [15] examined the laser- and thermally-induced decomposition of copper maleate and fumarate, and found different product distributions. Ethylene was the main gaseous product in the thermal-induced reaction whereas acetylene was the main product in the laser-induced reaction. The difference in products was attributed [15] to the faster heating rate in the laser-induced decomposition. Carr and Galwey [16] examined the isothermal decomposition of copper maleate and fumarate and identified CO<sub>2</sub> and CO as the main gaseous products. They observed a stepwise reduction of Cu(II) to Cu(I) and isomerization of the maleate into fumarate.

The decompositions of silver maleate and silver fumarate were studied to compare their thermal behaviour with those reported [13–16] for divalent transition-metal (nickel and copper) maleates and fumarates.

## Experimental

### *Material*

Silver maleate (denoted AgMt) was prepared by dissolving 5.96 g of maleic acid (Hopkin and Williams, England) in 200 ml of deionized water (at 60°C). A solution of 20.4 g of AgNO<sub>3</sub> (Chemapol, Czechoslovakia) in 200 ml of deion-

ized water was then added slowly, with continuous stirring, to the acid solution. A white precipitate of silver maleate was obtained, which was maintained in the precipitation bath for 3 h with continuous stirring (at 60°C). It was, then, filtered, washed with distilled water and dried at 100°C.

Silver fumarate (denoted AgFt) was prepared by a similar procedure, except that ethyl alcohol was used instead of water to dissolve the fumaric acid (Trade Int., Croydon, England).

Elemental analyses are shown in Table 1. The samples were also subjected to calcination at some selected temperatures (100–400°C). For clarity, the solid calcination products are denoted by the temperature applied. For example, AgMt (120) means the calcination products of silver maleate at 120°C.

**Table 1** Elemental analysis for both silver compounds

Compound	%C		%H		%Ag	
	Theor.	Found	Theor.	Found	Theor.	Found
AgMt	13.13	15.19	1.65	2.05	58.97	59.44
C <sub>4</sub> O <sub>4</sub> H <sub>2</sub> Ag <sub>2</sub> ·2H <sub>2</sub> O						
AgFt	14.57	14.60	0.61	0.69	65.42	66.67
C <sub>4</sub> O <sub>4</sub> H <sub>2</sub> Ag <sub>2</sub>						

### *Instrumentation and data processing*

X-ray diffractometry (XRD) of the two compounds and their solid phase decomposition products was carried out, using a model JSX-60 PA JEOL diffractometer (Japan) with Ni-filtered CuK $\alpha$  radiation. Diffraction patterns were matched with ASTM standard data.

The gas phase products were identified using infrared (IR) transmission spectra taken from the atmosphere surrounding a 0.5 g portion of the test sample, heated at 10 deg·min<sup>-1</sup> to various temperatures (100–400°C, for 10 min) in a specially designed IR-cell [17] with KBr windows. IR spectra of solid samples in KBr-discs were recorded between 4000–400cm<sup>-1</sup>.

60 MHz nuclear magnetic resonance (NMR) spectra with D<sub>2</sub>O mixed with DSS marker were used to monitor the isomerization of maleate into the more stable fumarate radical. The spectra were taken for the silver maleate and the solid products of decomposition at 250°C for 60 min. Identification was confirmed by adding the anion recognized and demonstrating an enhanced response for the specific peak, without the appearance of others.

Thermogravimetry (TG) and differential thermal analysis (DTA) were carried out on heating up to 500°C in a dynamic atmosphere of air (20 ml/min) and at four different heating rates ( $\varphi = 2, 5, 10$  and  $20 \text{ deg}\cdot\text{min}^{-1}$ ) using a model 30H Shimadzu thermal analyser (Japan). Typically, 10 to 15 mg samples were used with the TG and  $\alpha\text{-Al}_2\text{O}_3$  was the reference material for the DTA.

Values of the activation energy ( $E_a$ ) and frequency factor ( $\ln A$ ) were derived from the DTA results using the Kissinger method [18]. Plots of  $\ln \varphi/T_m^2$  vs.  $1/T$  were constructed and the slope and intercept values were used to derive  $E_a$  and  $\ln A$ .

## Results and discussion

### Thermal analysis

#### Silver maleate dihydrate (AgMt)

Figure 1 shows the TG curve for the decomposition of AgMt ( $\text{C}_4\text{H}_2\text{O}_4\text{Ag}_2\cdot 2\text{H}_2\text{O}$ ). The curve has four mass loss steps (I–IV), and a total mass loss of ca. 51.7% at  $\geq 310^\circ\text{C}$ . An initial, very small mass loss ( $< 1\%$ ) occurred between  $80\text{--}170^\circ\text{C}$ . This initial process is followed by step-I, between  $170\text{--}216^\circ\text{C}$ , which is accompanied by 25% mass loss. The subsequent step-II (at  $230\text{--}250^\circ\text{C}$ ), step-III (at  $250\text{--}304^\circ\text{C}$ ), and step-IV (at  $306\text{--}310^\circ\text{C}$ ) are accompanied by mass losses of 6, 17 and 3%, respectively.

The DTA curve for the decomposition of AgMt (Fig. 2) displays seven peaks at the following temperatures: 95 (exo), 133 (exo), 207 (endo), 245 (exo), 284 (exo), 300 (exo) and  $312^\circ\text{C}$  (exo). The first two peaks are weak, and the later three peaks overlap, with the  $300^\circ\text{C}$ -peak being the strongest feature displayed. The endotherm at  $207^\circ\text{C}$  is also strong, whereas the exotherm at  $245^\circ\text{C}$  is broad and weak.

The weak exotherms at 95 and  $133^\circ\text{C}$  correspond to the small mass loss (1%) detected in the TG curve (Fig. 1). They could be attributed to the elimination of some weakly bound surface species. The only endothermic peak (at  $207^\circ\text{C}$ ) corresponds very well to step-I in the TG curve, which is accompanied by 25% mass loss. It can be attributed to removal of water of hydration and, in part, to decomposition. The measured mass loss (25%) is much larger than would be expected (9.85%) for the removal of the two moles of water.

Table 2 indicates the shifts toward higher temperatures of the DTA maxima ( $T_{\text{max}}$ ) as a result of variations in the rate of heating ( $\varphi = 2, 5, 10$  and

**Table 2** Effect of heating rate ( $\phi$ ) on the DTA peak maxima ( $T_{\max}$ )

$\phi /$ deg.min <sup>-1</sup>	AgMt							AgFt			
	$T_{\max} / ^\circ\text{C}$							$T_{\max} / ^\circ\text{C}$			
	exo	exo	endo	exo	exo	exo	exo	exo	exo	exo	exo
	1	2	3	4	5	6	7	1	2	3	4
2	85	125	190	218	233	267	288	179	285	293	300
5	95	133	207	245	284	300	312	190	293	309	329
10	140	165	213	245	290	315	330	*	*	324	340
20	115	125	218	263	310	325	345	*	*	335	356

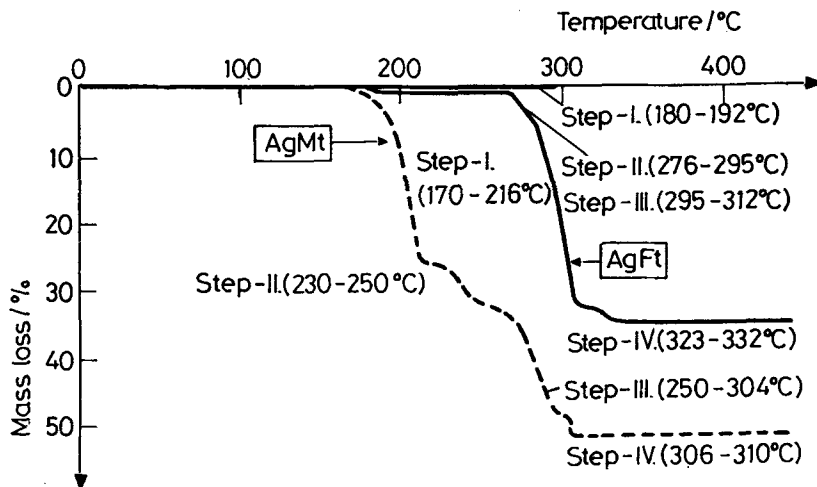
\*peaks that have disappeared on increasing the heating rate

20 deg.min<sup>-1</sup>) of AgMt. At 20 deg.min<sup>-1</sup>, the first two exotherms are shifted to lower temperatures.

Non-isothermal kinetic parameters ( $E_a$  and  $\ln A$ ) for the decomposition of AgMt, are listed in Table 3.

#### Anhydrous silver fumarate AgFt

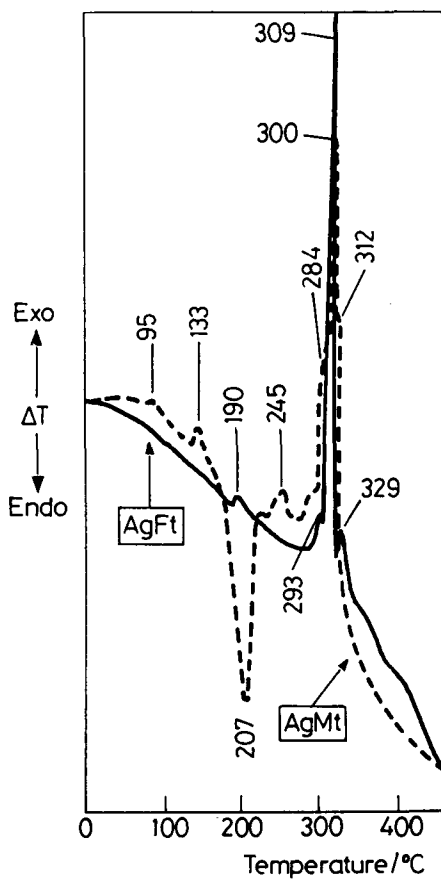
The TG curve for AgFt is shown in Fig. 1. There are four mass loss steps (I–IV). The total mass loss measured at  $\geq 340^\circ\text{C}$  is 36.5%. Step-I takes place between 180 and 192°C, and is accompanied by a small mass loss of about 1%.



**Fig. 1** TG curves obtained in air (20 ml/min) for silver maleate dihydrate (----) and anhydrous silver fumarate (—) at a heating rate of 5 deg.min<sup>-1</sup>

**Table 3** Non-isothermal kinetic parameters for the decomposition of silver maleate dihydrate (AgMt) and anhydrous silver fumarate (AgFt) obtained using the Kissinger method [18]

Kinetic parameter	AgMt					AgFt	
	Process number					Process number	
	3	4	5	6	7	3	4
	Dehydration	Decomposition				Decomposition	
$E_a/\text{kJ}\cdot\text{mol}^{-1}$	139±8	101±5	63±2	139±7	105±6	143±8	113±6
$\ln A/\text{min}^{-1}$	34±2	23±2	12±1	27±3	20±2	28±3	21±2
Correl. coeff.	0.965	0.996	0.997	0.966	0.997	0.998	0.986

**Fig. 2** DTA curves obtained in air (20 ml/min) for silver maleate dihydrate (----) and anhydrous silver fumarate (—) at a heating rate of  $5\text{ deg}\cdot\text{min}^{-1}$

Step-II commences at 276–295°C with a mass loss of about 4%. Step-III, which overlaps with step-II, represents a major event. It is accompanied by 28.5% mass loss (at 295–312°C). The fourth, and final, step-(IV) takes place between 323 and 332°C, and involves a mass loss of 2.5–3%.

The DTA curve for AgFt (Fig. 2) reveals the occurrence of four exothermic processes maximized at 190, 293, 309 and 329°C. The first, very small, exotherm (ca. 190°C) corresponds to the TG step-I (mass loss 1%), and can be attributed to elimination of some adsorbed species. The second exotherm (ca. 293 °C) corresponds to step-II in the TG curve (Fig. 1). The third exotherm (ca. 309°C) corresponds to step-III, which is accompanied by 28.5% mass loss. The last exotherm, maximized at 329°C, is related to step-IV in the TG curve (Fig. 1) which is accompanied by 2.5–3% mass loss.

The shifts experienced by the DTA peak maxima ( $T_{\max}$ ) as a result of variation in the rate of heating ( $\phi = 2, 5, 10$  and  $20 \text{ deg}\cdot\text{min}^{-1}$ ) are shown in Table 2. The first two exothermic peaks disappeared when the rate of heating exceeded  $5 \text{ deg}\cdot\text{min}^{-1}$ .

The non-isothermal kinetic parameters ( $E_a$  and  $\ln A$ ) are listed in Table 3 for peaks 3 and 4. The activation energy values calculated for AgFt are very close to those calculated for the last two processes (6 and 7) for AgMt.

### *Product analysis*

#### Solid phase products

##### (a) X-ray diffraction

XRD analysis of both salts and their calcination products showed that above 290°C, both salts gave an identical pattern which matches well the standard pattern of silver metal (ASTM card 4–783). Therefore, silver metal is proved to be the final decomposition product of AgMt and AgFt.

##### (b) Infrared spectroscopy

IR spectra of the solid decomposition products of AgMt showed some characteristic bands of undecomposed AgMt at  $1660\text{--}1385 \text{ cm}^{-1}$  of  $\nu\text{-C=C}$  and  $\nu\text{-C=O}$  for cisoid-transoid forms [19],  $670 \text{ cm}^{-1}$  ( $\delta\text{-C-H}$ ) and  $3700\text{--}3000 \text{ cm}^{-1}$  ( $\nu\text{-C-H}$ ) up to 150°C. This agrees with the TG results (step-1, Fig. 1), that AgMt is stable at 150°C apart from sublimation. Similarly, IR spectra showed also the characteristic absorption bands of the parent AgFt up to 220°C. This agrees with the TG results (Fig. 1) which indicated that AgFt is stable at 220°C except for slight sublimation.

## (c) NMR analysis

Figure 3 displays NMR spectra for the parent AgMt and its solid phase decomposition product at 250°C for 60 min. For AgMt, the spectrum (a) monitors a singlet response at  $6.00 \pm 0.05$  ppm in addition to the solvent ( $D_2O$ ) response at 4.7 ppm. The peak appearing at 6.00 ppm is assignable to the two equivalent hydrogen atoms in the maleate anion [16]. The absence of any other responses is a strong evidence for the high purity of the reactant.

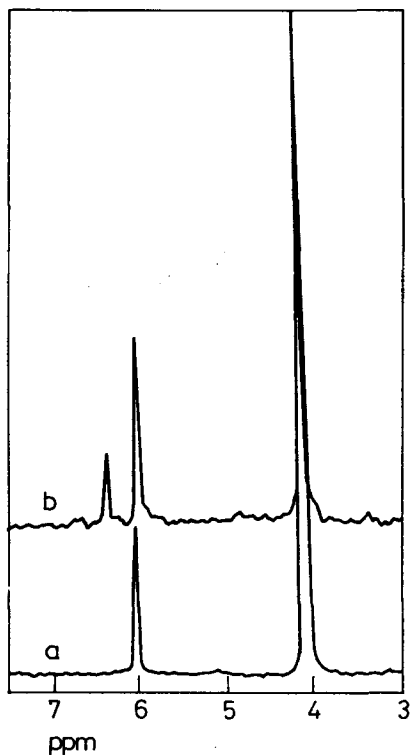


**Fig. 3** NMR responses of (a) silver maleate dihydrate and (b) its calcination product at 250°C for 60 min (in air) dissolved in  $D_2O$

For AgMt (250°C), on the other hand, the NMR spectrum (b) shows the emergence of another peak at  $6.5 \pm 0.05$  ppm, which can be attributed to the fumarate anion [16]. This peak was found to increase with increasing decomposition temperature at the expense of the maleate peak (at 6.00 ppm).

NMR results support the observation shown in Fig. 1, that above 230°C the thermal decomposition behaviours of AgMt and AgFt are largely similar. The net mass loss determined in the TG curve of AgMt (i.e. 35%) at > 230°C, is very close to that (36%) shown by AgFt over the same temperature range. Thus, we

can conclude from the TG measurements and the NMR results that the maleate radical is transformed into fumarate (isomerization) at 230°C.

### Gaseous products

#### a) AgMt

IR spectra of the gaseous decomposition products on heating AgMt at 120, 230 and 350°C, for 10 min, are exhibited in Fig. 4. The spectra are dominated by the characteristic absorptions of maleic anhydride (at 1856, 1781, 1290, 1242, 1060, 898, 873, 840 and 697  $\text{cm}^{-1}$ ) [20]. Their intensities increase with calcination temperature. Characteristic absorptions of  $\text{CO}_2$  (between 620–730  $\text{cm}^{-1}$  and 2330–2370  $\text{cm}^{-1}$  [21]) are observed in the 120°C-spectrum. They grow stronger with temperature increase. A weak absorption at 2147  $\text{cm}^{-1}$ , due to slight proportions of CO, can be observed in the 120°C-spectrum. Its intensity increases gradually with temperature increase up to 350°C and then weakens appreciably on further heating to 400°C. The spectra reveal the formation of an appreciable amount of ethylene (absorptions at 3120, 1980, 1930 and 990  $\text{cm}^{-1}$  [22]) at 230°C, which increases further at 300 and 350°C, but decreases on heating above 350°C.

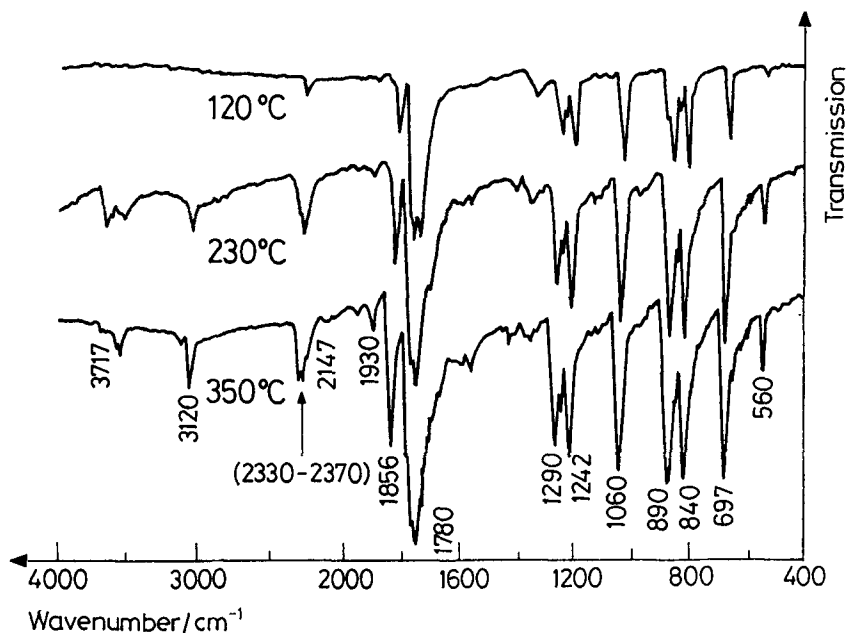


Fig. 4 IR spectra of the gaseous products released upon heating silver maleate at the temperatures indicated for 10 min in air

In addition to the above identified gaseous decomposition products, weak absorptions due to traces of acetone ( $1094$  and  $1750\text{ cm}^{-1}$ ) [22], ethyl alcohol (at  $2900\text{ cm}^{-1}$ ) and acetaldehyde (at  $2950$  and  $1724\text{ cm}^{-1}$ ), can also be resolved in the spectra obtained on heating at  $350^\circ\text{C}$ .

#### b) AgFt

IR spectra of the gaseous decomposition products of AgFt at  $150$ ,  $250$ ,  $300$  and  $350^\circ\text{C}$  are shown in Fig. 5. Maleic anhydride can be identified in the spectra taken following heating at  $150$ ,  $250$ ,  $300$  and  $350^\circ\text{C}$  for 10 min. Its proportion is, however, less than that in the gaseous products of decomposition of AgMt (Fig. 4). Characteristic absorptions of  $\text{CO}_2$  and  $\text{CO}$  (identified above) can also be seen. The proportion of  $\text{CO}_2$  increases with calcination temperature (from  $150$ – $350^\circ\text{C}$ ). The proportion of  $\text{CO}$  decreases with temperature.

Ethylene, acetone and traces of acetylene were also identified in the spectrum recorded at  $250^\circ\text{C}$ . Their proportions increased slightly at  $300$  and  $350^\circ\text{C}$ .

The formation of methane ( $1310$  and  $910\text{ cm}^{-1}$ ) and isobutene ( $890\text{ cm}^{-1}$ ) can be identified [23] in the gaseous products of decomposition of both silver compounds. These two gaseous products could be produced from acetone in a surface-catalyzed bimolecular reaction [24], which indicates that such a sur-

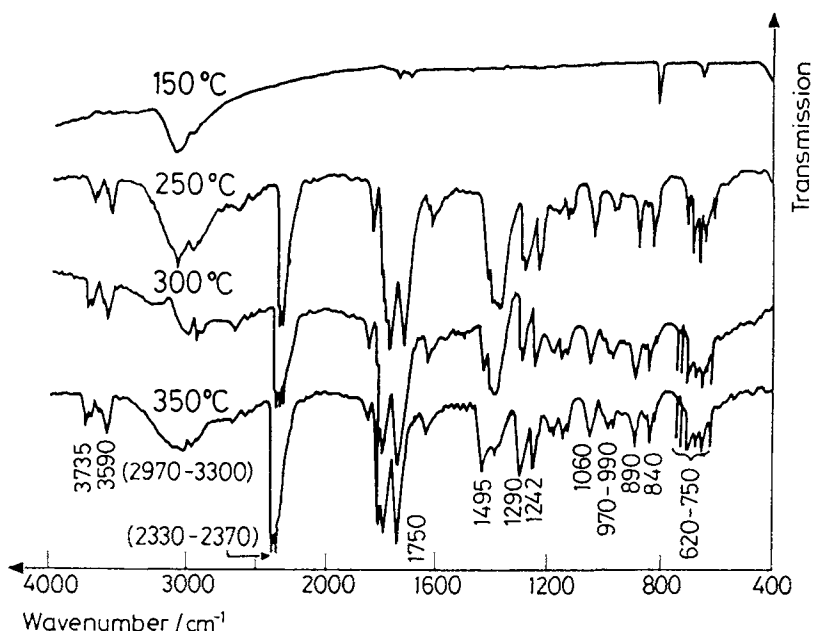


Fig. 5 IR spectra of the gaseous products released upon heating silver fumarate at the temperatures indicated for 10 min in air

face-catalyzed reaction (over silver metal) is occurring during the decomposition of both silver compounds.

The spectrum recorded at 150°C shows some absorption at 825 cm<sup>-1</sup> (assignable to trans H-C=C-H [22]) and 3000–3300 cm<sup>-1</sup> (assignable to the ionized carboxyl group [22]). This supports the TG results (Fig. 1), in showing that AgFt suffers no appreciable decomposition at that temperature, except for a slight sublimation of the parent compound.

The gaseous decomposition products are thus not different from those identified for the decomposition of silver maleate dihydrate, except that the distribution of these products may be different. This, in fact, supports the TG, DTA and X-ray results, which all show that both compounds react similarly, especially at high temperatures, due to the conversion of the maleate anion into the more stable fumarate anion (above 250 °C).

## Conclusions

The decomposition pathways of the two silver compounds can be summarized as follows:

AgMt and AgFt undergo an initial sublimation and desorption of some physically adsorbed species (Figs 1, 2, 4 and 5) at 120°C (for AgMt) and 180°C (for AgFt). This is followed by dehydration and some decomposition of anhydrous AgMt at 207°C (see DTA, Fig. 2). The exothermic transformation of the maleate anion into the more stable fumarate anion, together with partial decomposition to yield Ag<sub>2</sub>O oxide and maleic anhydride, takes place at 245°C (Fig. 2).

Above 245°C, the thermal behaviours of the two compounds are very similar. The remaining three overlapping, exothermic peaks (Fig. 2) are identical for both silver compounds. In the TG curves, steps III and IV for the two salts are similar. Values of  $E_a$  for the two exothermic processes for both salts are almost equal.

The reduction of silver oxide, possibly by CO gas, to produce Ag metal and CO<sub>2</sub> is represented by exotherms at 284°C (AgMt) and at 293°C (AgFt). Catalytic reactions on the freshly generated surfaces of silver metal (formed in the previous step) are accompanied by exothermic peaks at 300°C (AgMt) and at 309°C (AgFt). The final exotherms at 312°C (AgMt) and 329°C (AgFt) represent the oxidation of CO to form CO<sub>2</sub>.

The results obtained here are similar to those reported for copper maleate and fumarate [16] in that both systems exhibit maleate isomerization into fumarate. This was not reported for the analogous nickel compounds [15] although

both compounds produced ethylene and traces of acetylene which is similar to our results.

\* \* \*

We thank Professor M. I. Zaki of Minia University (Egypt) for critical reading of the manuscript and the very useful discussion during the accomplishment of this work.

## References

- 1 M. E. Brown, D. Dollimore and A. K. Galwey, *Comprehensive Chemical Kinetics*, Vol. 22. Reactions in the Solid State, Elsevier, Amsterdam 1980.
- 2 A. Keller and F. Korosy, *Nature (London)*, 162 (1948) 580.
- 3 A. Finch, P. W. M. Jacobs and F. C. Tompkins, *J. Chem. Soc.*, (1954) 2053.
- 4 V. V. Boldyrev, V. I. Eroshkin, I. A. Ryzhak and L. M. Kefeli, *Dokl. Akad. Nauk SSSR*, 173 (1967) 117.
- 5 R. M. Haynes and D. A. Young, *Discuss. Faraday Soc.*, 31 (1961) 229.
- 6 A. K. Potapovich, V. V. Sviridov, G. A. Branitskii and V. N. Makatun, *Teor. Eksp. Khim.*, 3 (1967) 375.
- 7 A. G. Leiga, *J. Phys. Chem.*, 70 (1966) 3254, 3260.
- 8 A. K. Galwey and M. A. Mohamed, *J. Chem. Soc., Faraday Trans. I*, 81 (1985) 2503.
- 9 A. K. Galwey, M. A. Mohamed and P. J. Herley, *J. Chem. Soc., Faraday Trans. I*, 84(3) (1988) 729.
- 10 A. K. Galwey, M. A. Mohamed and M. E. Brown, *J. Chem. Soc., Faraday Trans. I*, 84(1) (1988) 57.
- 11 M. E. Brown, H. Kelly, A. K. Galwey and M. A. Mohamed, *Thermochim. Acta*, 127 (1988) 139.
- 12 R. J. Acheson and A. K. Galwey, *J. Chem. Soc. (A)*, 1968, 942.
- 13 M. J. McGinn, B. R. Wheeler and A. K. Galwey, *Trans. Faraday Soc.*, 67 (1971) 1480.
- 14 M. J. McGinn, B. R. Wheeler and A. K. Galwey, *Trans. Faraday Soc.*, 66 (1970) 1809.
- 15 K. Taki, P. H. Kim and S. Namba, *Bull. Chem. Soc. of Japan*, 43 (1970) 1450.
- 16 N. J. Carr and A. K. Galwey, *J. Chem. Soc., Faraday Trans. I*, 84(5), 1988, 1357.
- 17 J. B. Peri and R. B. Hannan, *J. Phys. Chem.*, 64 (1960) 1526.
- 18 H. E. Kissinger, *J. Anal. Chem.*, 29 (11) 1957, 1702.
- 19 S. F. Dyke, A. J. Floyd, M. Sainsbury and R. S. Theobald, *Organic Spectroscopy. An Introduction* (2nd ed.), Longman, London 1978.
- 20 K. G. R. Tachler, F. Matlok and H. U. Gremlich, *Merck FTIR Atlas*, VCH Publisher, Weinheim 1988, p. 122.
- 21 S. A. A. Mansour, M. A. Mohamed and M. I. Zaki, *Thermochim. Acta*, 129 (1988) 187.
- 22 R. L. Pecsok, L. D. Shields, T. Cairns and I. G. McWilliam, 'Modern Methods of Chemical Analysis', 2nd ed., John Wiley Inc., New York 1976.
- 23 H. M. Ismail, *J. Anal. Appl. Pyrolysis*, 21 (1991) 315.
- 24 M. I. Zaki and N. Sheppard, *J. Catal.*, 80 (1982) 114.

**Zusammenfassung** — Mittels TG und DTA wurde in einer dynamischen Luftatmosphäre bis zu 500°C die nichtisotherme Zersetzung von Silbermaleat-Dihydrat ( $C_4H_2O_4Ag_2 \cdot 2H_2O$ ) und von

wasserfreiem Silberfumarat ( $C_4H_2O_4Ag_2$ ) untersucht. Vor dem Einsetzen der Zersetzung (bei  $170^\circ C$  für Silbermaleat und bei  $280^\circ C$  für Silberfumarat) zeigen beide Verbindungen etwas Sublimationsverhalten (bei  $120^\circ C$  für Silbermaleat und bei  $180^\circ C$  für Silberfumarat).

Unter Einsatz von IR-Spektroskopie wurden die gasförmigen Zersetzungsprodukte beider Verbindungen hauptsächlich als Maleinsäureanhydrid und  $CO_2$  identifiziert, daneben wurde in geringeren Mengen auch Ethylen, Ethylalkohol, Aceton, Methan und Isobuten festgestellt. Wie durch Röntgendiffraktion festgestellt wurde, ist metallisches Silber das feste Endprodukt der Zersetzung. Zur Verfolgung der Umwandlung des Maleatradikales in das stabilere Fumarat oberhalb von  $230^\circ C$  wurde NMR-Analyse eingesetzt. Aus dem Effekt der Aufheizgeschwindigkeit (2, 5, 10 und  $20 \text{ deg}\cdot\text{min}^{-1}$ ) auf die DTA-Messungen wurden die kinetischen Parameter ( $E_a$  und  $A$ ) berechnet.

Anhand der erhaltenen Resultate und auch aufgrund der Ähnlichkeit mit analogen Systemen wurde ein Mechanismus für die Reaktionswege der Zersetzung vorgeschlagen.